Development of NiMH-based Fuel Cell/Battery (FCB) system: Characterization of Ni(OH)$_2$/MnO$_2$ positive electrode for FCB

Bokkyu Choi, Sunmook Lee, Chihiro Fushimi, Atsushi Tsutsumi *

Collaborative Research Center for Energy Engineering, Institute of Industrial Science, The University of Tokyo, 4-6-1 Komaba, Meguro-ku, Tokyo 153-8505, Japan

ARTICLE INFO

ABSTRACT

The performance of the positive electrode composed of a mixture of nickel hydroxide (Ni(OH)$_2$) and a small amount of manganese dioxide (MnO$_2$) was investigated for the positive electrode of Fuel Cell/Battery (FCB) system. It was found that the positive electrode can function not only as an active material of secondary batteries when it is charged but also as a catalyst of fuel cells when oxygen is supplied, which was confirmed by the following characterization: electrochemical characterization was performed with cyclic voltammetry (CV) and galvanostatic discharge curve in oxygen and oxygen-free atmosphere. CV of Ni(OH)$_2$/MnO$_2$ positive electrode exhibited the redox reaction of Ni(OH)$_2$ as well as oxygen reduction reaction. It was observed that the discharge curves of positive electrode had two working potentials in half cell test when the electrode was charged and oxygen was supplied: one from the reactions of nickel oxyhydroxide (NiOOH); the other from the fuel cell reactions of manganese dioxide (MnO$_2$). It was also observed that the discharge curves had two working voltages in full cell test when the cell was fully charged and oxygen was supplied: one at 1.2 V from the battery reactions of NiOOH; the other at 0.8 V from the fuel cell reactions of MnO$_2$. In particular, the discharge capacity of overcharged cell was improved approximately 2 times compared with a battery of the same electrode quantity due to the additional function of this system as a fuel cell by using oxygen generated by water electrolysis. XRD analysis showed that there was no crystal structure change before and after (over)charge–discharge cycles. In summary, these experimental results showed that the novel bi-functional FCB system could provide an improved overall energy density per weight compared with conventional secondary batteries.

© 2009 Elsevier B.V. All rights reserved.

1. Introduction

Natural energy sources, such as solar power and wind power, have attracted a great deal of attention for the last few decades due to the tremendous increase in the price of petroleum oil, the major fossil fuel comprising a critical portion of the overall energy supply [1,2]. These natural energies have the following advantages: (i) they are renewable and so help solve energy shortage problems; (ii) it can reduce global warming due to no emission of carbon dioxide [3]. However, natural energy sources have the intrinsic problem of the non-stable energy supply because they strongly rely on the climate change [4]. One solution to overcome such problem and to supply stable energy with natural power sources is to construct a high-capacity power storage system such that the power should be stored when power generation is more than power consumption (e.g. during the night time) and the stored power will be supplied

when power demand is more than power supply (e.g. during the day time).

Secondary batteries are an excellent candidate for such electrical power storage system because its theoretical exergy efficiency of electric energy is 100% as well as it can store and produce electric power multiple times, which leads to the improved total energy efficiency. However, the capacity of secondary batteries is determined by the total amount of the electrode, which implies that when energy larger than the battery capacity is supplied, the extra energy would be transformed to thermal energy and cannot be stored for useful energy.

Apart from batteries, fuel cells are one of the most attractive power generation systems due to their fascinating features such as high power generation efficiency (theoretical efficiency $\eta = \Delta G/\Delta H = 83\%$, 25 °C) compared with that of the conventional internal combustion engine (15–25%) and clean energy such that fuel cell produce only water without emitting carbon dioxide [5]. Similar to batteries, the basic components of fuel cells are positive electrode/electrolyte/negative electrode. However, the energy density of fuel cells is approximately 10 times larger than that of

batteries through the supply of fuels due to the different functions of the electrode materials. For example, in case of alkaline fuel cell, hydrogen and oxygen are supplied from the external storage source into the negative and positive electrodes, in which the reduction and oxidation of fuels occur due to the catalytic activities of the electrode materials [6]. In contrast, batteries generate electric power by reduction and oxidation reaction of electrode materials.

In the view of the above, the enhancement of the energy density of secondary batteries is expected by a novel bi-functional Fuel Cell/Battery (FCB) system, which can function both as a secondary battery without fuel supply and also as a fuel cell with fuel supply [7,8]. To construct this novel bi-functional Fuel Cell/Battery (FCB) system, electrode materials should satisfy the following requirements:

Negative electrode: electrochemical redox reaction in low potential and hydrogen oxidation reaction.

Positive electrode: electrochemical redox reaction in high potential and oxygen reduction reaction.

There are several types of secondary batteries such as lead–acid, nickel–cadmium (NiCd), lithium-ion, and nickel–metal hydride (NiMH) secondary batteries [9,10]. In the current study, NiMH secondary batteries have been chosen for FCB system due to the following advantages: (i) 1.2 V of working voltage, comparable to NiCd batteries and/or dry cells; (ii) environmentally acceptable and recyclable; (iii) safe in overcharging and overdischarging; (iv) high energy density compared with NiCd secondary batteries and dry cells.

Details of the electrochemical reactions of NiMH-based FCB system as shown in Fig. 1 are as follows:

First, FCB system can store energy by charging the electrode.

Positive electrode:

$$Ni(OH)_2 + OH^- \leftrightarrow NiOOH + H_2O + e^- \tag{1}$$

Negative electrode:

$$M + H_2O + e^- \leftrightarrow MH + OH^- \tag{2}$$
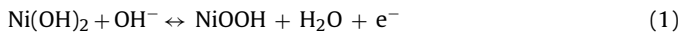
Upon complete charging of the respective electrodes, water electrolysis would occur and generate hydrogen on the negative

electrode side and oxygen on the positive electrode side, which would be stored in the gas tanks.

Positive electrode:

$$4OH^- \rightarrow O_2 + 2H_2O + 4e^- \tag{3}$$

Negative electrode:

$$4H_2O + 4e^- \rightarrow 4OH^- + 2H_2 \tag{4}$$

Stored energies in the gaseous form in this way can produce electric energy through the reverse reaction of water electrolysis when discharged by the fuel cell function of the FCB system. Therefore, this novel bi-functional NiMH-based FCB system can possess significantly improved energy capacity.

As mentioned above, the electrodes of FCB system should be bi-functional as catalysts of fuel cell and as active materials of secondary battery. It has been reported that metal hydride, the negative electrode of NiMH battery, can be charged by hydrogen gas and oxides simply by electrochemical reaction [11,12].

Charged by H_2 gas:

$$2M + xH_2 \leftrightarrow 2MH_x \tag{5}$$

Discharged by an electrochemical reaction

$$2MH_x + xOH^- \leftrightarrow 2M + xH_2O + xe^- \tag{6}$$
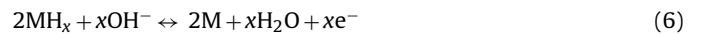
Therefore, metal hydride (MH) is compatible with the negative electrode of FCB system. Although MH has absorption and desorption capabilities of hydrogen, those of oxygen are not acquired with nickel hydroxide ($Ni(OH)_2$), the positive electrode material. Thus, our current research attempted to resolve this problem by fabricating the positive electrode with a mixture of $Ni(OH)_2$ and a small amount of manganese dioxide (MnO_2), a well-known oxygen reduction catalyst [12–14]. Based on these, this paper investigated the electrochemical performance of $Ni(OH)_2/MnO_2$ positive electrode of NiMH-based FCB system.
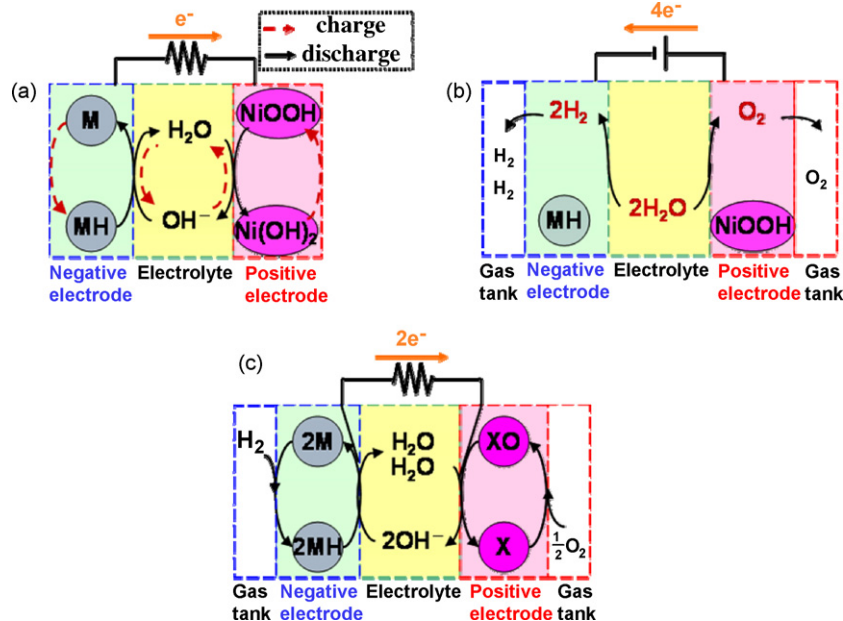

Fig. 1. Operational principle of NiMH-based Fuel Cell/Battery (FCB) system: (a) secondary battery mode; (b) electrolysis mode (when overcharged); (c) fuel cell mode.

2. Experimental

2.1. Fabrication of electrodes

2.1.1. Negative electrodes

Negative electrodes were fabricated using spherical metal hydride particles (Kawasaki Heavy Industries, Ltd.) with 0.5–1.7 mm in diameter. The composition of lanthanum–nickel–metal hydride and ethylene–vinyl acetate (EVA) was 98:2 (w/w). This mixture was transferred onto nickel foam (20 mm in diameter), followed by pressing at 6 MPa for 10 min. This was then soaked in 6 M KOH aqueous solution.

2.1.2. Positive electrodes

$Ni(OH)_2$ positive electrodes (Kawasaki Heavy Industries, Ltd.) were also fabricated using particles with 0.5–1.7 mm in diameter. The positive electrodes were composed of $Ni(OH)_2$, MnO_2, carbon black (CB) and ethylene–vinyl acetate (EVA) with 9:1:3:1 of mass ratio. CB and EVA were playing a role as a conductive material and a binder, respectively. This mixture was transferred onto nickel foam (20 mm in diameter), followed by pressing at 6 MPa for 10 min. This was then soaked in 6 M KOH aqueous solution.

2.2. Experimental apparatus and electrochemical measurement

2.2.1. Half cell test

A schematic illustration of the experimental cell assembly and experimental apparatus in the Fuel Cell/Battery (FCB) half cell test is shown in Figs. 2 and 3, respectively. Electrochemical measurements were carried out in a three-electrode cell with 0.4 g fabricated positive electrode (thickness: 1.0 mm) as working electrode, nickel foam as counter electrode and carbon electrode (Micro Inc., Japan) as reference electrode. The electrolyte was prepared with polypropylene sheet which was preincubated in 6 M KOH aqueous solution. Oxygen gas and argon gas were supplied into the experimental cell with compressed oxygen cylinder and argon cylinder. For the comparison, the half cell test in 6 M KOH aqueous solution was also conducted in a three-electrode cell with 0.4 g fabricated positive electrode (thickness: 1.0 mm) as working electrode, nickel foam as counter electrode and Ag/AgCl/saturated KCl (RE-1C, BAS Inc.) as reference electrode. This three-electrode cell was also used for the activation of metal hydride.
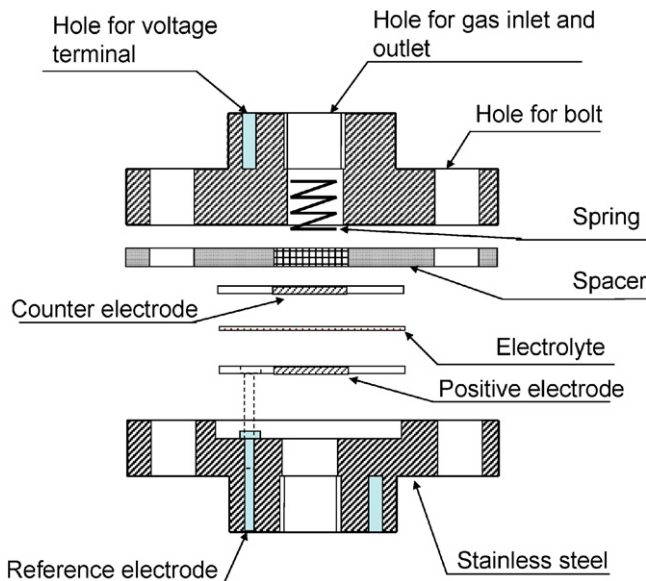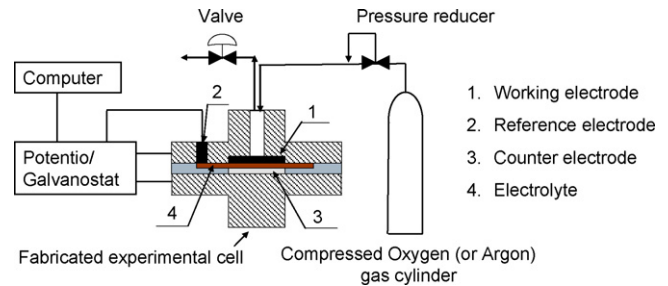

Fig. 3. Schematic diagram of the experimental apparatuses of NiMH-based Fuel Cell/Battery (FCB) test.

2.2.2. Full cell test

In case of the full cell test of Fuel Cell/Battery (FCB) under gaseous oxygen supply, the full cell was composed of 1.0 g of MH negative electrode and 0.4 g of $Ni(OH)_2/MnO_2$ positive electrode with the experimental cell as shown in Fig. 2. A schematic illustration of the experimental cell assembly in the full cell test of Fuel Cell/Battery (FCB) under overcharging condition is shown in Fig. 4. The experimental cell was assembled with 0.1 g fabricated positive electrode (thickness: 0.6 mm) and 1.0 g fabricated negative electrode (thickness: 1.0 mm). The electrolyte was prepared with alkaline polymer gel electrolyte in the following way: first, 10 wt% of potassium of cross-linked poly(acrylic acid) in 6 M KOH aqueous solution was prepared. Next, the polymer gel was incubated in vacuum for over 3 days at room temperature. It was reported that cross-linked poly(acrylic acid) gel electrolyte has a high ionic conductivity and wide potential almost comparable to KOH aqueous solution [15,16].

2.3. Characterization

Cyclic voltammograms (CV) and galvanostatic performance were obtained with Analytical 1480 Multistat (Solartron) at 25 °C in oxygen gas and argon gas. The crystal structure changes of the positive electrode were observed with XRD (XRD miniflex, Rigaku Corporation) at a scan rate of $1°\,min^{-1}$ within $2\theta = 5$–$90°$.

3. Results and discussion

3.1. Electrochemical properties of $Ni(OH)_2/MnO_2$ positive electrode in half cell assembly

Fig. 5 shows the cyclic voltammograms of the positive electrode fabricated with the $Ni(OH)_2/MnO_2$ positive electrode under oxygen and argon atmosphere, respectively. Purge of experimen-
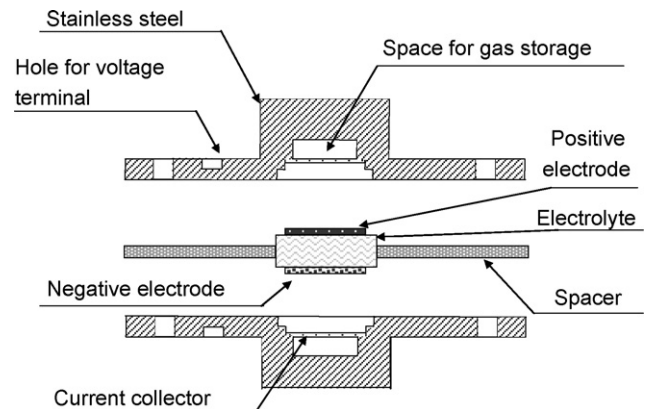

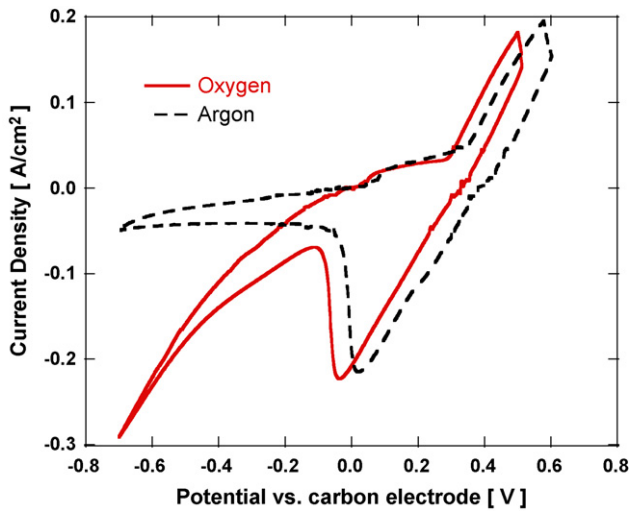**Fig. 2.** Cell assembly of NiMH-based Fuel Cell/Battery (FCB) in the half cell test.

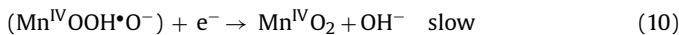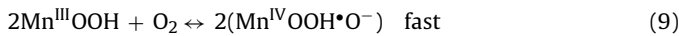**Fig. 4.** Cell assembly of NiMH-based Fuel Cell/Battery (FCB) in the full cell test.
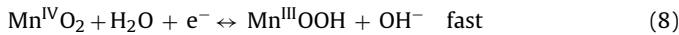
Fig. 5. Cyclic voltammograms of the Ni(OH)$_2$/MnO$_2$ positive electrode oxygen gas (solid line) and argon gas (dashed line) at 0.2 MPa and 298 K, respectively. Scan rate: 5 mV s^{-1}.

Fig. 6. Discharge behavior of the Ni(OH)$_2$/MnO$_2$ positive electrode (at the discharged state) under 0.2 MPa oxygen (solid line) and argon (dashed line) atmosphere at 0.2 C discharge rate and 298 K, respectively.

tal cell was conducted with oxygen gas or argon gas at 500 ml/min of flow rate and 0.2 MPa of fluid pressure for 30 min. After purge, the exit valve of the cell was closed and the CV measurements of positive electrode were conducted at 0.2 MPa of oxygen or argon atmosphere.

In case of argon atmosphere, there were only two peaks; one peak at 0.5 V from the oxidation of nickel hydroxide; the other at 0 V from the reduction of nickel oxyhydroxide as shown in Eq. (7).

$$Ni(OH)_2 + OH^- \leftrightarrow NiOOH + H_2O + e^- \qquad (7)$$
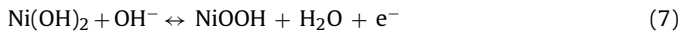
On the other hand, the cyclic voltammogram under oxygen atmosphere exhibited an additional peak at more negative potential region than the reduction peak of nickel oxyhydroxide due to the oxygen reduction reaction (ORR). This indicates the positive electrode possesses the reduction capability of oxygen by manganese dioxide. The ORR mechanism of MnO$_2$ catalyst has been reported as follows [12–14]:

$$Mn^{IV}O_2 + H_2O + e^- \leftrightarrow Mn^{III}OOH + OH^- \quad fast \qquad (8)$$

$$2Mn^{III}OOH + O_2 \leftrightarrow 2(Mn^{IV}OOH \bullet O^-) \quad fast \qquad (9)$$

$$(Mn^{IV}OOH \bullet O^-) + e^- \rightarrow Mn^{IV}O_2 + OH^- \quad slow \qquad (10)$$

Overall reaction

$$O_2 + 2H_2O + 4e^- \rightarrow 4OH^- \qquad (11)$$

In the first step of oxygen reduction, MnO$_2$ is discharged and transforms to MnOOH such as Eq. (8). Then, MnOOH reacts with oxygen and returns to MnO$_2$ through (9) and (10) reactions. Eventually, oxygen reduction takes place on the positive electrode, which is the fuel cell reaction such as Eq. (11).

Galvanostatic discharge test was also performed under oxygen and argon atmosphere at 0.2 C discharge rates in order to investigate the discharge performance of Ni(OH)$_2$/MnO$_2$ positive electrode at 0% state of charge (SOC). Fig. 6 shows that the potential of the positive electrode dropped rapidly within 10 min in case of argon atmosphere whereas the potential of the positive electrode steadily remained at −0.13 V for more than 1 h in case of oxygen atmosphere. This indicates that the positive electrode of the NiMH-based FCB system possessed the ORR for fuel cell reaction as aforementioned reactions (8)–(11). FCB performance of the positive electrode was also investigated through the galvanostatic discharge test under 0.2 MPa oxygen atmosphere when the positive electrode was fully charged, which was compared with the discharge performance of
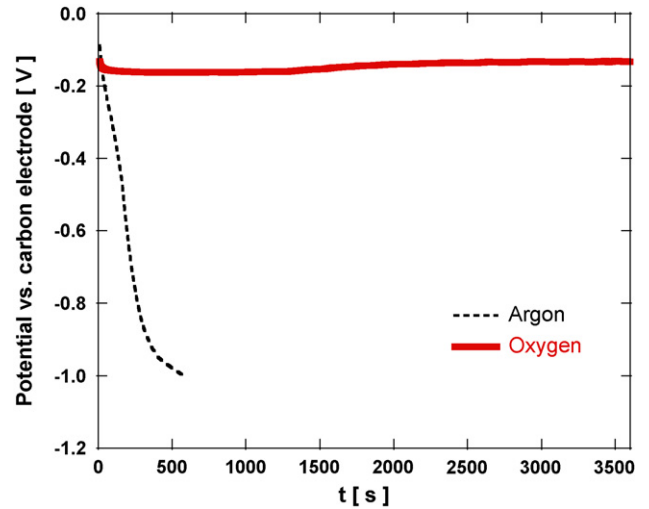
positive electrode conducted in 6 M KOH aqueous solution in order to estimate the effect of oxygen gas. Fig. 7 shows the potential discharge behavior of the positive electrode under oxygen atmosphere and 6 M KOH aqueous solution, respectively. It was observed that the discharge curve under oxygen atmosphere had two working potentials whereas the discharge curve in 6 M KOH aqueous solution had only one working potential. In case of the discharge curve with oxygen, the ORR started to occur upon the termination of the reduction reaction of nickel oxyhydroxide. Note that the potential of oxygen reduction is in good agreement with the result in Fig. 6. Therefore, it can be concluded that the Ni(OH)$_2$/MnO$_2$ positive electrode can function not only as a positive electrode in secondary batteries when it is charged, but also as a catalyst in a positive electrode of fuel cells when it is discharged and oxygen is supplied. In addition, it was found that the discharge capacities did not reach 100% DOD (depth of discharge) in the current research. It is attributed to the relatively thick electrode layer, which was aimed for a better contact of the electrode materials with the fuel gas but resulted in a poor discharge capacities of the first working potential in secondary battery mode.
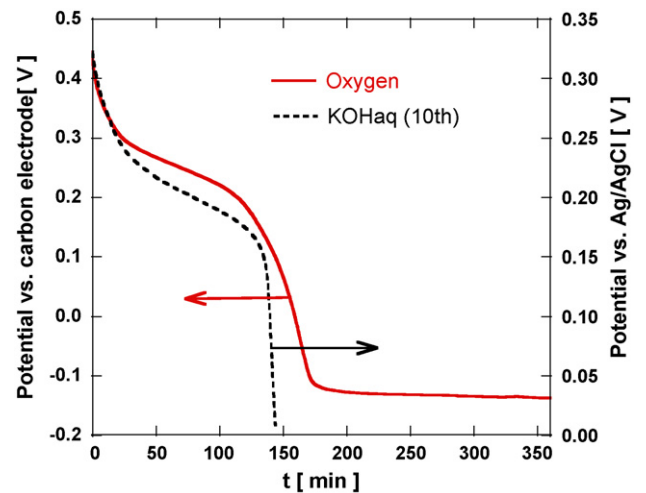

Fig. 7. Discharge behavior of the positive electrode (at the charged state) under oxygen atmosphere (solid line) and 6 M KOH aqueous solution (dashed line) at 0.2 C discharge rate and 298 K, respectively.

3.2. Electrochemical properties of $Ni(OH)_2/MnO_2$ positive electrode in full cell assembly

3.2.1. Oxygen gas supply

Full cell performance in oxygen atmosphere through the continuous oxygen gas supply into the cell was examined by galvanostatic discharge test with the cell assembly shown in Fig. 2. The full cell was composed of 1.0 g of MH negative electrode and 0.4 g of $Ni(OH)_2/MnO_2$ positive electrode. Initial activation of electrode was conducted with 6 M KOH aqueous solution by 0.2 C, 10 charge–discharge cycles in the half cell apparatus. After activation, the electrode was fully charged and used for fabricating the full cell. And then, purge of experimental cell was conducted with oxygen gas in the positive electrode and with argon gas in the negative electrode, respectively, at 500 ml min^{-1} of flow rate and 0.2 MPa for 30 min. After purge, the exit valve of the cell was closed and 0.2 C of galvanostatic discharge was conducted. Fig. 8 shows the galvanostatic discharge behavior of the fabricated full cell when the positive electrode was in 0.2 MPa oxygen atmospheres. There were two working voltages in discharge curve at 1.2 V and 0.8 V. In addition, it was also found that the potential from the oxygen reduction reaction of manganese dioxide after the reduction reaction of nickel oxyhydroxide steadily remained at −0.1 V, which corresponds to the discharge of fuel cell. This also confirms that FCB system using $Ni(OH)_2/MnO_2$ positive electrode can function both as a secondary battery and as a fuel cell.

3.2.2. Overcharging

To investigate the discharge performance of overcharged cell, the experimental cell as shown in Fig. 4 was fabricated and connected with the experimental apparatus. The theoretical capacity of the fabricated cell was calculated from the amount of $Ni(OH)_2$ of the positive electrode because the mass ratio of negative electrode (1.0 g) to positive electrode (0.1 g) was 10:1, under which condition the overcharging reaction was limited by the positive electrode. In this condition, oxygen would be only generated when the cell is overcharged less than 10 times of theoretical capacity because hydrogen would be absorbed in metal hydride. After assembling the experimental cell, 5 charge/discharge cycles were run at a rate of 0.2 C for the initial activation of electrodes. Fig. 9 shows the charge and discharge performances of complete cell test with the electrode
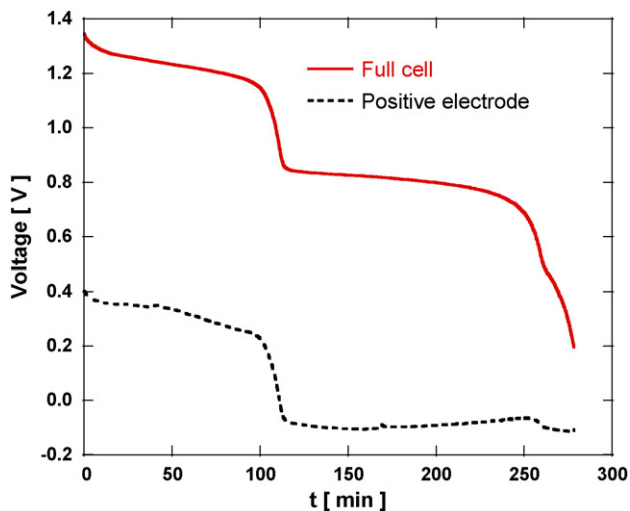

Fig. 8. Galvanostatic discharge behavior of the fabricated cell (solid line) at 0.2 C discharge rates. Argon and oxygen gases were supplied to the negative and positive electrodes at 0.2 MPa and 298 K, respectively. The dashed line shows the potential behavior of the positive electrode during the discharge reaction of the fabricated cell.
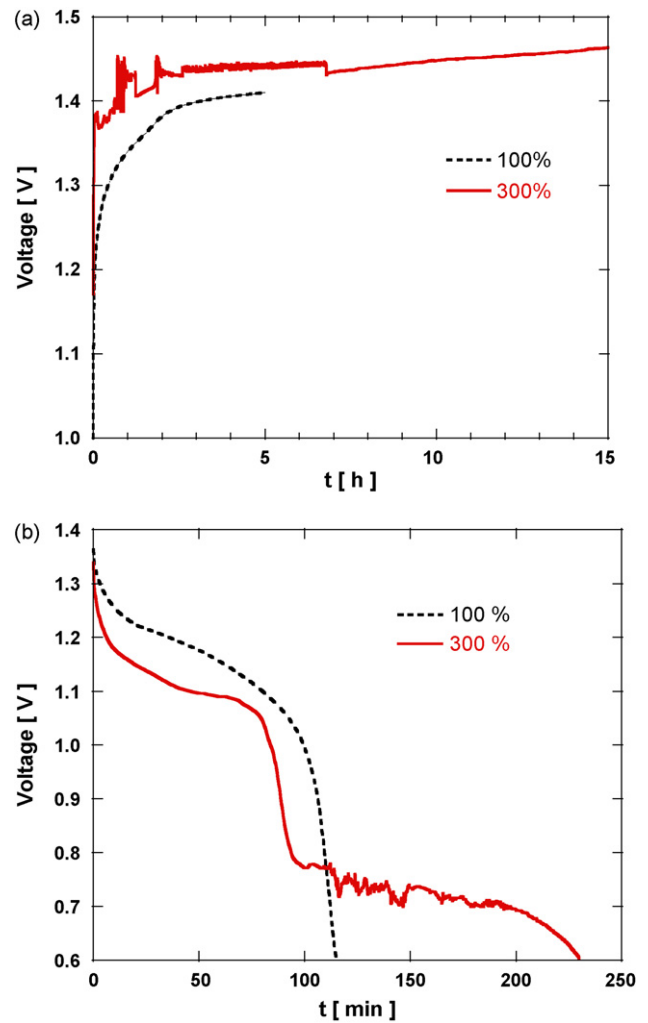

Fig. 9. Discharge curves of complete cell test with fabricated positive electrode consisting of a mixture of $Ni(OH)_2$ and MnO_2 with different SOCs: (a) charge curves; (b) discharge curves.

consisting of a mixture of $Ni(OH)_2$ and MnO_2 for different SOCs. At this time, the cut-off voltage of discharge was 0.6 V. In case of SOC 100%, the potential steadily decreased, which is typical of a secondary battery discharge curve. After this, the cell was overcharged 3 times larger (SOC 300%) than the theoretical charge capacity of positive electrode and then was discharged at 0.2 C. The discharge capacity of SOC 300% was approximately 2 times larger than that of SOC 100%. It should be noted that the discharge curve of SOC 300% has two plateaus, one at 1.1 V and the other at 0.8 V. This can be attributed to the bi-functional characteristics of this system: 1.1 V of working voltage from the battery performance by the reduction of NiOOH; 0.8 V of working voltage from the fuel cell performance by the reduction of oxygen by MnO_2. This indicates that the cell functioned as a fuel cell during the period of the second plateau by using the oxygen generated from the electrolysis of water.

3.3. XRD characterization of the electrode

XRD patterns of the positive electrode were compared before and after the (over)charge/discharge experiments as shown in Fig. 10. It has been reported that MnO_2 converts into electrochemically stable Mn_3O_4 simultaneously with the reduction reaction if MnO_2 functions as an active material of the positive electrode [7,17]:

$$MnO_2 + H_2O + e^- \leftrightarrow MnOOH + OH^- \tag{12}$$
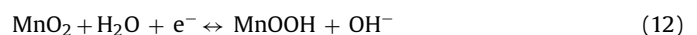
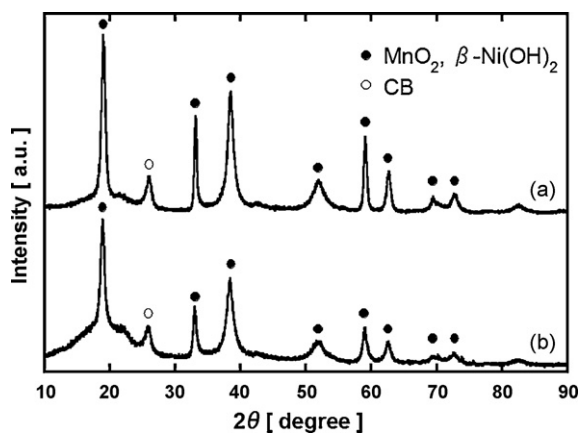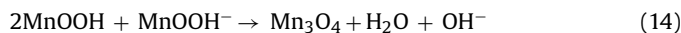**Fig. 10.** XRD patterns for fabricated positive electrode consisting of a mixture of Ni(OH)$_2$ and MnO$_2$: (a) before charge/discharge cycles; (b) after overcharge/discharge cycles.

$$MnOOH + e^- \rightarrow MnOOH^- \qquad (13)$$

$$2MnOOH + MnOOH^- \rightarrow Mn_3O_4 + H_2O + OH^- \qquad (14)$$

It was found from the XRD results that there was no change in the structure of the positive electrode and no formation of Mn$_3$O$_4$, an inhibitor of MnO$_2$ catalytic activity, indicating that MnO$_2$ was not involved in the above reactions but functioned only as an oxygen reduction catalyst.

4. Conclusion

A positive electrode fabricated with the mixture of nickel hydroxide and a small amount of manganese dioxide (9:1 w/w) was tested for the positive electrode of Ni/MH-based Fuel Cell/Battery (FCB) system. Cyclic voltammograms and galvanostatic discharge curves under oxygen and argon atmosphere indicated that the positive electrode can function not only as a positive electrode of secondary batteries when it is charged, but also as a catalyst in a positive electrode of fuel cells when oxygen is supplied and the nickel oxyhydroxide was reduced to nickel hydroxide. It was observed that the discharge curves had two working voltages when the cell was fully charged and oxygen was supplied: one at 1.2 V from the battery reactions of NiOOH; the other at 0.8 V

from the fuel cell reactions of MnO$_2$. In particular, the overcharged cell exhibited approximately 2 times larger discharge capacity compared with that of a battery with the same electrode quantity due to the additional function of this system as a fuel cell by using oxygen generated by water electrolysis. XRD analysis showed that there was no crystal structure change before and after (over)charge–discharge cycles, which indicated that MnO$_2$ only functioned as oxygen reduction catalyst but was not involved in the transformation of Mn$_3$O$_4$, the inhibitor of the catalytic activity of MnO$_2$.

References

[1] E. Regnier, Energy Economics 29 (2007) 405–427.
[2] A.M. Omer, Renewable Sustainable Energy Reviews 12 (2008) 2265–2300.
[3] J. Miliken, F. Joseck, M. Wang, E. Yuzugullu, Journal of Power Sources 172 (2007) 121–131.
[4] H. Ibrahim, A. Ilinca, J. Perron, Renewable Sustainable Energy Reviews 12 (2008) 1221–1250.
[5] L. James, D. Andrew, Fuel Cell Systems Explained. second ed., 2003.
[6] T. Burchardt, P. Gouerec, E. Sanchez-Cortezon, Z. Karichev, J.H. Miners, Fuel 81 (2002) 2151–2155.
[7] S. Lee, B. Choi, N. Hamasuna, C. Fushimi, A. Tsutsumi, Journal of Power Sources 181 (2008) 177–181.
[8] B. Choi, S. Lee, H. Kawai, C. Fushimi, A. Tsutsumi, International Journal of Hydrogen Energy 34 (2009) 2058–2061.
[9] R.M. Dell, Solid State Ionics 134 (2000) 139–158.
[10] F. Beck, P. Rüetschi, Electrochimica Acta 45 (2000) 2467–2482.
[11] B. Sakintuna, International Journal of Hydrogen Energy 32 (2007) 1121–1140.
[12] Y.L. Cao, H.X. Yang, X.P. Ai, L.F. Xiao, Journal of Electroanalytical Chemistry 557 (2003) 127–134.
[13] K. Matsuki, H. Kamada, Electrochimica Acta 31 (1986) 13–18.
[14] M.L. Calegaro, F.H.B. Lima, E.A. Ticianelli, Journal of Power Sources 158 (2006) 735–739.
[15] C. Iwakura, S. Nohara, N. Furukawa, H. Inoue, Solid State Ionics 148 (2002) 487–492.
[16] C. Iwakura, K. Ikoma, S. Nohara, N. Furukawa, H. Inoue, Journal of the Electrochemical Society 150 (12) (2003) A1623–A1627.
[17] J. McBreen, in: D.H. Collin (Ed.), Power Sources, vol. 5, Academic Press, London, 1975, p. 31.